Assessing climate change impacts on flood frequency and magnitude using CMIP6 GCMs: a case study of the Likhu River in eastern Nepal

Bipin Gurung, Sabina Budhathoki, Shirapa Mahaju, Utsav Raj Pandey, Subash Dhakal, Govind Acharya
Department of Civil Engineering, Sagarmatha Engineering College, Tribhuvan University, Lalitpur, Nepal

Abstract

Floods are becoming more severe with climate change disrupting the hydrological cycle, undermining the reliability of the historical flood records for future projections. Despite considerable research on large river basins, small to medium-sized basins like Nepal's Likhu River remain under-researched, particularly in integrating CMIP6 climate models and Shared Socioeconomic Pathways (SSPs). To the best of the authors' knowledge, this is the first study to apply the CMIP6/SSP framework to a medium-sized Himalayan basin in eastern Nepal, addressing a critical gap in regional climate-hydrology research. This study aims to quantify the future changes in flood magnitude and frequency of the Likhu River basin by linking CMIP6 climate models with an integrated hydrological-statistical approach. Five selected CMIP6 Global Climate Models (GCMs) under SSP245 and SSP585 scenarios were incorporated to drive a calibrated and validated Hydrologic Engineering Center's Hydrologic Modeling System (HEC-HMS) model, with flood frequency analysis performed using Log-Pearson Type III and Generalized Extreme Value (GEV) distributions. The future floods for each GCM and an ensemble model were evaluated for the three time periods: Near Future (2025–2050), Mid Future (2051–2075), and Far Future (2076–2100). Our findings suggest that a 100-year return-period flood estimated using the historical data may occur more frequently, with recurrence intervals shortening to 5–25 years under future climate change scenarios, highlighting the impact of climate change. Results also point out the variability among the different GCMs and necessitate the use of multiple GCMs to capture the range of uncertainties in flood predictions. These findings demonstrate that current design standards and practices for water-related structures need further modifications and improvements to provide safeguards against future flow conditions as monsoon extremes intensify.

Keywords: climate change, CMIP6, GCMs, SSPs, HEC-HMS, flood frequency analysis

1 Introduction

Floods, driven by extreme weather events, are environmental threats that pose catastrophic consequences, including massive economic damage, destruction of infrastructure and property, and loss of life [1, 2]. Between 2000–2023, about 45% of all worldwide disasters were triggered by rainfall-induced floods [3, 4]. These events are often ascribed to extreme weather events disrupting the hydrological cycle, thus altering precipitation patterns and leading to frequent flooding [5]. Moreover, rising temperature as a result of climate change and variability increases the probability of extreme weather events [6]. Additionally, IPCC [7] has published evidence that recent climate change has had a notable influence on flood magnitude and frequency of occurrence across global regions.

Nepal, ranking 11^{th} globally in terms of overall disaster vulnerability and 2^{nd} among flood-prone countries in South Asia, experiences frequent, devastating floods, particularly during the monsoon season that generally lasts from June to September [8].Recent studies have begun to document the intensification of hydroclimatic extremes specifically in eastern Nepal and the broader Koshi basin. Lutz et al. [9] projected consistent

increases in runoff from High Asian river basins driven by accelerated glacier melt and increasing precipitation under future warming scenarios, with particular implications for Nepal's eastern river systems. Similarly, research reviewed by Bharati et al. [10] suggests that wet seasons in the Koshi basin are likely to become wetter, with an increasing frequency of high-flow events and severe rainfall. These regional trends are compounded by projected temperature increases of approximately 1.0–2.2°C by mid-century across High Asian basins, which are expected to further intensify the monsoon hydrological cycle and elevate flood risk in mountainous sub-basins such as the Likhu River [9, 11]. Recent years have witnessed major impacts, with 927 flood incidents claiming 260 lives between mid-2018 and mid-2024, including catastrophic events like the September 2024 floods [12]. According to Kafle [13], huge damage in the downstream reach of the country and in India has occurred from several past floods in the Koshi Basin. According to Bhattarai et al. [14], extreme flows in Nepal occur between June and September, accounting for about 80% of the total annual values, with peaks generally occurring during July and August. Understanding the characteristics of floods, such as their magnitude and frequency of occurrence, is imperative for planners and managers who aim to construct water-resilient infrastructure. Hydraulic structures, for instance, are constructed by incorporating knowledge of different flood events of different return periods [2, 15].

However, climate change is expected to exacerbate the frequency and severity of flooding events, which may result in the destruction of water-related infrastructure [16]. As a result, researchers have developed Global Circulation Models (GCMs) to facilitate the simulation of current and future climate predictions [17]. GCMs consist of sophisticated mathematical equations to replicate the dynamic processes of various components of the Earth's climate system, such as the atmosphere, seas, and terrestrial surface, at the global scale [18]. GCMs are often combined with different emission scenarios to project future climate changes. IPCC [7] introduced Shared Socioeconomic Pathways (SSPs) in AR6 (Sixth Assessment Report) that describe how socioeconomic factors like population growth, economic development, and technological progress might influence greenhouse gas emissions, adaptation, and mitigation challenges, further paired with Representative Concentration Pathways (RCPs), levels of radiative forcing (in watts per square metre).

While GCMs combined with scenarios like SSPs provide projections for future climate, their application to climate change-induced flood assessment remains limited in Nepal. Existing studies primarily rely only on historical streamflow data, neglecting future climate projections. For example, Bhattarai et al. [14] and Acharya and Joshi [15] utilized historical data for analysis but lacked integration of future climate change. Furthermore, research disproportionately focuses on large rivers despite evidence that smaller to medium river systems are also vulnerable to changing climate [19]. As emphasized by Sheng et al. [20], small to medium-sized river basins possess limited buffering capacity to temporarily store excess water, making them sensitive to intense rainfall and more vulnerable to flooding, yet they remain understudied. Medium-sized basins differ fundamentally from large river systems in their hydrological behaviour. Unlike large basins, where the spatial averaging of precipitation and the network of tributaries provides significant attenuation of peak flows, medium-sized basins exhibit faster hydrological response times, shorter concentration periods, and limited in-channel and floodplain storage capacity [21, 22]. These characteristics make them particularly susceptible to flash flooding triggered by intense, short-duration monsoon precipitation, a phenomenon increasingly documented in the Hindu Kush-Himalayan region [23]. Furthermore, the steep topographic gradients and thin soils typical of mid-hill Himalayan catchments like the Likhu basin reduce infiltration capacity, amplifying surface runoff generation and accelerating the translation of precipitation pulses into high-discharge flood events [10, 24].

The study evaluates flood magnitude and frequency changes across three future time horizons—Near

Future (2025–2050), Mid Future (2051–2075), and Far Future (2076–2100)—using daily hydrometeorological observations and CMIP6 climate model projections under SSP245 and SSP585 scenarios. Hydrological simulation is performed using the Hydrologic Engineering Center's Hydrologic Modeling System (HEC-HMS) [25], with subsequent flood frequency analysis utilizing Log-Pearson Type III and GEV distributions. The findings are intended to be applicable not only to the Likhu basin but also to serve as a methodological reference for hydrological impact assessments in comparable data-scarce, medium-sized river basins across the Hindu Kush-Himalayan region.

This study aims to address critical gaps and offers contributions to flood assessment under climate change in Nepal's Likhu River, a medium-sized basin in eastern Nepal, in the following ways:

1. Shifting attention from Nepal's large rivers to a less-studied and medium-sized river system.
2. Incorporating precipitation and temperature projections from five specific CMIP6 GCMs to project future flood simulations.
3. Quantifying the potential alterations in both the magnitude and frequency of extreme flood events under projected climate scenarios.
4. Developing a practicable methodology by integrating climate projections with hydrological modeling and statistical analysis to quantify climate-attributed shifts in design flood events.

2 Material and Methods

The methodological framework of this research was broadly categorized into four distinct sections: data collection, data analysis, hydrological modeling, and interpretation to assess future flood risks. The study began with the collection of various datasets. Climate data were extracted and bias-corrected to reduce systematic errors in climate model outputs [26], and five suitable GCM models were selected based on performance evaluation to project future precipitation and temperature. Similarly, the hydrological model was set up using time-series, discharge, and spatial data, followed by calibration and validation using standard performance evaluation criteria [27]. Subsequently, goodness-of-fit tests were conducted to identify the most appropriate statistical distribution. The calibrated model was then used to simulate future streamflow. Finally, flood frequency and magnitude analyses were performed using the projected hydrological data to interpret future flood scenarios. The overall methodological framework of the current research has been schematically presented in Figure 1.

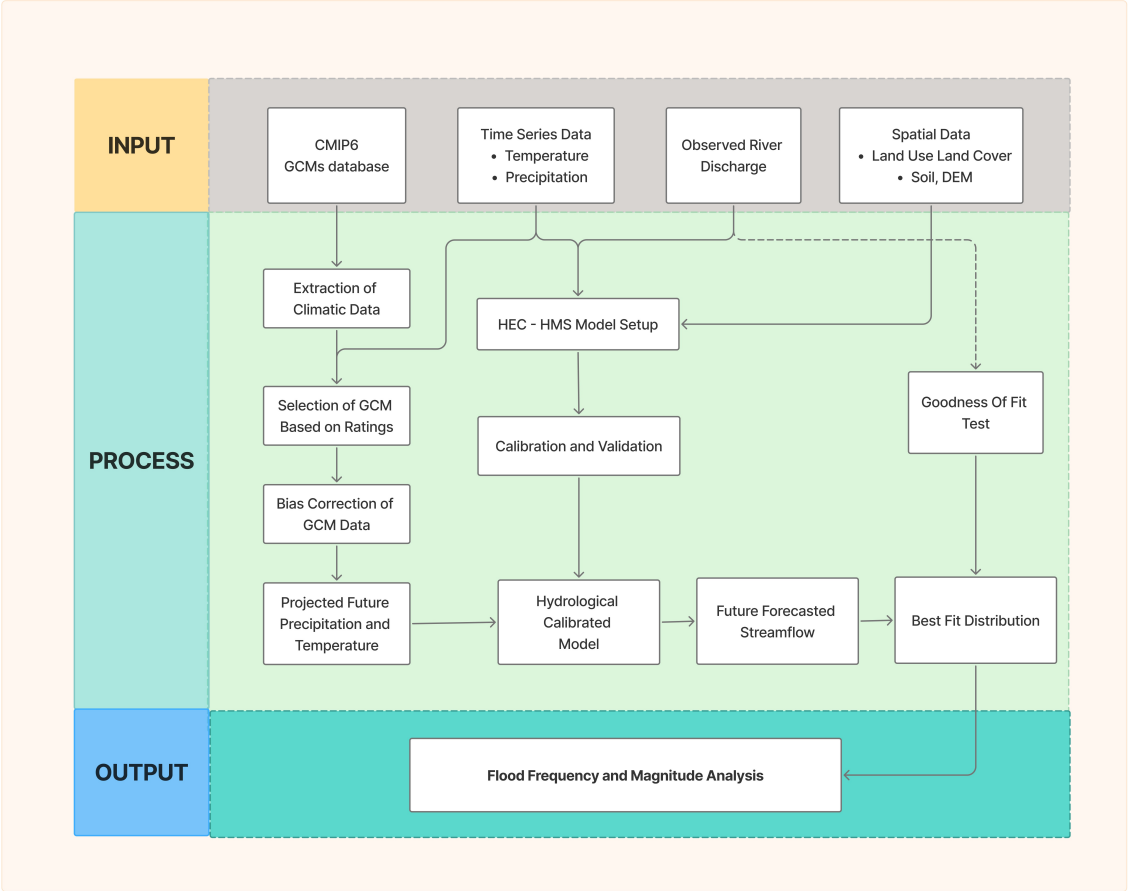

Figure 1. Methodological framework of the research.

2.1 Study area

Originating from the downstream reach of the snowcapped Likhu Dhuni Mountain, the Likhu River is a tributary of the Sun Koshi River which is one of the seven major tributaries of the Sapta Koshi River in Nepal. The basin's catchment area has been delineated using topographic data derived from a 12.5 m spatial Digital Elevation Model (DEM) and it covers an area of 849 km^2 (Figure 2). The DEM has been obtained from the Alaska Satellite Facility (ASF) and has been processed in a GIS environment using ArcGIS. The catchment's elevation ranges from 494 to 6,819 m above mean sea level.

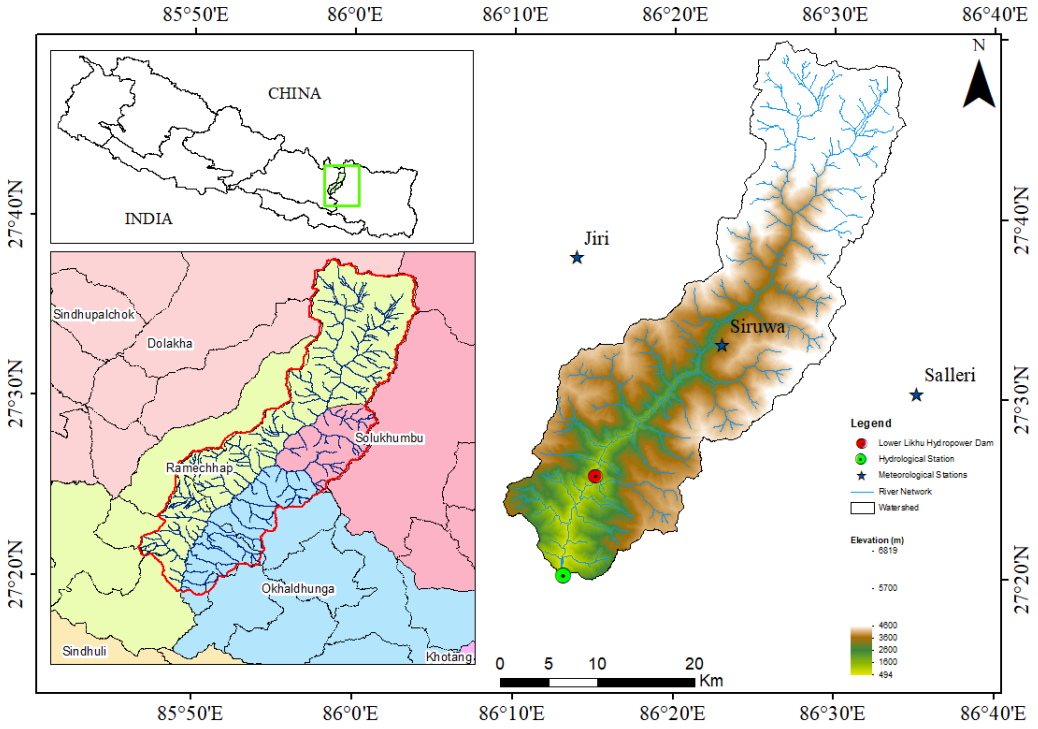

Figure 2. Study area showing elevation, river network, and hydrological and meteorological stations within the catchment.

2.2 Data

Table 1 presents details on the types, characteristics and sources of datasets used in the study. It includes information on geospatial, time-series and climate model data appropriate for hydrological modeling. Three meteorological stations located within and near the study basin (Table 2) and a hydrological station located at the catchment's outlet (Table 3) were employed in this study.

Table 1. Data sources used in the study.

Dataset	Data type	Description	Source
Terrain dataset	Geospatial grid	Digital elevation model (DEM), 12.5 m × 12.5 m	Alaska Satellite Facility (ASF)
Land use/land cover	Spatial grid	Land-cover raster, 10 m × 10 m resolution	Esri Land Cover, Living Atlas
Soil	Geospatial vector	Soil classification	SOTER (Soil and Terrain) database
Precipitation and temperature	Time series	Daily observed records	DHM, Nepal
River discharge	Time series	Daily observed records	DHM, Nepal
Global climate models (GCMs)	Climate-model output	Bias-corrected CMIP6 daily precipitation and temperature projections	World Climate Research Programme

Table 2. DHM meteorological stations used in the study.

S.N.	Index no.	Station name	Location	Latitude (N)	Longitude (E)	Elevation (m)	Data availability
1	1103	Jiri	Dolkha	27.63	86.23	1877	1985–1989
2	1219	Salleri	Solukhumbu	27.51	86.58	2383	1985–1989
3	1224	Siruwa	Solukhumbu	27.55	86.37	1614	1973–2020

Table 3. DHM hydrological station used in the study.

S.N.	Station no.	River name	Location	Latitude (N)	Longitude (E)	Elevation (m)	Data availability
1	660	Likhu	Sangutar	27°20'10"	86°13'10"	828	1966–2006

The available station records contained gaps due to instrument failure and inconsistent observation periods (Tables 2 and 3). These were addressed prior to model setup using standard infilling techniques. For precipitation, the Normal Ratio Method was applied, which weights data from neighboring stations proportionally by their mean annual precipitation, making it particularly suitable for stations in topographically varied terrain such as the Likhu basin where rainfall gradients are significant. For temperature, the Linear Regression Method was employed using Siruwa station, the only station with a near-complete record (1973–2020), as the reference, given the strong linear relationship between temperature observations at neighboring stations at similar elevations. The infilled records were then subjected to consistency checks using double-mass curve analysis before being used as model inputs.

2.3 Climate Change Projection

Researchers have developed bias-corrected datasets of daily precipitation, maximum and minimum temperatures using output from the 13 GCMs that participated in the Coupled Model Intercomparison Project Phase 6 (CMIP6), considering the climate change impacts in South Asia. The 13 GCMs were shortlisted based on the availability of daily precipitation, maximum and minimum temperatures [28]. They used empirical quantile mapping (EQM) to develop bias-corrected data at daily temporal and 0.25° spatial resolution for six countries in South Asia (India, Pakistan, Bangladesh, Nepal, Bhutan, and Sri Lanka). The data were acquired from the World Climate Research Programme website for our study. The CMIP6-GCMs data were downloaded under two scenarios, SSP245 and SSP585, and extracted to the station level using R Studio.

Among them, the five best GCMs were selected based on the evaluation of the performance rating by comparing Nash-Sutcliffe Efficiency (NSE), the Ratio of Root Mean Square Error to the Standard Deviation of Observations (RSR), and the Percentage Bias (PBIAS). In our current study, climatic data for the two specific SSPs were selected: SSP 245 and SSP 585. SSP 245 corresponds to an intermediate GHG emissions scenario and radiative forcing of about 4.5 W/m^2 by 2100; on the other hand SSP 585 corresponds to a high-emission scenario with radiative forcing of about 8.5 W/m^2 by 2100.

Table 4. Performance rating criteria for GCM selection.

Performance	NSE	RSR	PBIAS	Rating
Very good	$0.75 < \text{NSE} \leq 1.00$	$0 \leq \text{RSR} \leq 0.50$	$\lvert\text{PBIAS}\rvert < 10$	5
Good	$0.65 < \text{NSE} \leq 0.75$	$0.50 < \text{RSR} \leq 0.60$	$10 \leq \lvert\text{PBIAS}\rvert < 15$	4
Satisfactory	$0.50 < \text{NSE} \leq 0.65$	$0.60 < \text{RSR} \leq 0.70$	$15 \leq \lvert\text{PBIAS}\rvert < 25$	3
Unsatisfactory	$0.40 < \text{NSE} \leq 0.50$	$0.70 < \text{RSR} \leq 0.80$	$25 \leq \lvert\text{PBIAS}\rvert < 35$	2
Poor	$\text{NSE} \leq 0.40$	$\text{RSR} > 0.80$	$\lvert\text{PBIAS}\rvert \geq 35$	1

Sources: Moriasi et al. [27] and Baral et al. [29].

Table 5. Selected GCMs used in the analysis.

S.N.	Model name	Research centre
1	ACCESS-ESM1-5	Australian Community Climate and Earth System Simulator (ACCESS)
2	BCC-CSM2-MR	Beijing Climate Center, China Meteorological Administration, China
3	CanESM5	Canadian Centre for Climate Modelling and Analysis, Canada
4	EC-Earth3-Veg	European Community Earth System Model consortium
5	INM-CM4-8	Institute for Numerical Mathematics (INM)

GCMs, however, have limitations on regional assessment as GCMs are characterized by coarse resolution having pixel size of approximately 250 to 600 km. They fail to capture fluctuations in local climatic parameters [30]. According to Grotch and MacCracken [31], data remain relatively coarse in resolution and are unable to resolve significant sub-grid scale features. Such limitations are to be addressed through bias correction prior to applying into hydrological studies at regional or local scales [26]. Among the various available bias correction methods, different techniques are generally recommended for temperature and precipitation owing to the fundamentally different statistical properties of these variables. For temperature, which exhibits an approximately symmetric, near-Gaussian distribution, the linear transformation approach is well-established as an effective and parsimonious approach [26]. For precipitation, which is characterized by a skewed distribution, intermittency, and heavy tails, nonparametric quantile mapping has been demonstrated to outperform simpler linear methods, particularly in capturing the extremes of the distribution that are most relevant to flood studies [26, 32]. Gudmundsson et al. [32] compared multiple statistical bias correction methods for precipitation and concluded that quantile mapping approaches consistently achieved superior performance in reproducing observed distributional characteristics, including extreme values. Similarly, Chen et al. [33] emphasized that applying distribution-appropriate correction methods separately to temperature and precipitation yields more reliable hydrological impact projections than using a single uniform approach. Accordingly, in this study, the linear transformation approach was applied to temperature and nonparametric quantile mapping was applied to precipitation, following established best practices for climate-hydrology impact assessments at the basin scale.

2.4 Hydrological modelling

2.4.1 Model setup

We employed HEC-HMS for hydrologic simulation by integrating three main components: a Basin Model, a Meteorologic Model, and Control Specifications. There are 7 sub-basins, 5 junctions, and 5 reach elements present in the basin (Figure 3). The model was calibrated using the data between 1982 and 1984 and its performance was assessed using statistical metrics, including the NSE, PBIAS, and RSR; the calibrated model

was then validated for 1985–1986. The calibration (1982–1984) and validation (1985–1986) periods are admittedly short, a constraint directly attributable to the limited availability of continuous discharge records at the rural Sangutar gauging station (Station 660) in our study. However, short calibration periods are a widely recognized challenge in data-scarce mountainous regions and have been adopted in numerous peer-reviewed studies without compromising the reliability of model projections [34, 35]. Perrin et al. [36] demonstrated that even approximately 350 days of streamflow data can yield acceptable model parameter estimates when the period encompasses a representative range of hydrological conditions. In this study, the calibration years encompass contrasting conditions, with 1984 representing a high-flow year and 1982–1983 representing comparatively moderate flow years, thereby ensuring the model parameters were exposed to a meaningful range of catchment responses. Furthermore, the model performance statistics indicate good performance, as the NSE values of 0.69 and 0.71 for calibration and validation, respectively, meet the "Good" performance threshold defined by Moriasi et al. [27]. Similar short-record approaches have been successfully employed in HEC-HMS-based studies across the Himalayan region [13].

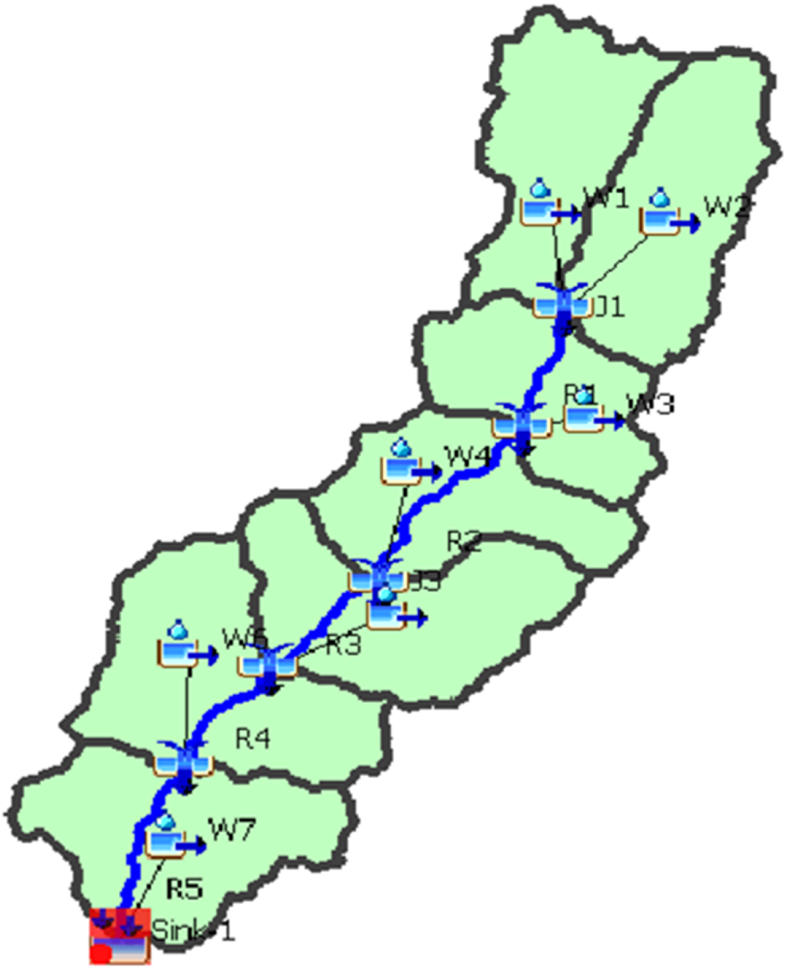

Figure 3. Basin model in HEC-HMS.

2.4.2 Future Flow Projection

Future flow projections of the river flow discharge were undertaken for three timeframes of Near Future (2025–2050), Mid Future (2051–2075), and Far Future (2076–2100). Climate variables from the GCM

outputs under SSP 245 and SSP 585 scenarios were integrated into the calibrated and validated HEC-HMS model. The model was then executed for each GCM and an Ensemble model under both scenarios to simulate discharge patterns.

2.4.3 Flood Frequency Analysis

Before conducting the flood analysis, EasyFit software was used to determine the best fitting probability distribution which is a comprehensive software system designed for parameter estimation and data fitting in various types of mathematical models, including those involving probability distributions [37]. For analysis, the annual peak daily flood discharge data were used rather than instantaneous ones. The annual peak daily flood discharge data for the period 1980–2014 were obtained to use in several distribution methods: Normal, Lognormal, Log-Pearson III, Gumbel Max, and GEV. Goodness-of-fit tests (Kolmogorov-Smirnov, Anderson-Darling, and Chi-Square) at a 0.05 significance level were used to evaluate distribution performance, where Log-Pearson Type III and GEV were identified as the most suitable distribution methods (Table 6).

Table 6. Results of the goodness-of-fit test.

S.N.	Distribution	Kolmogorov-Smirnov			Anderson-Darling			Chi-squared		
		Critical Value at 0.05 = 0.23788			Critical Value at 0.05 = 2.5018			Critical Value at 0.05 = 7.8147		
		Statistic	Reject	Rank	Statistic	Reject	Rank	Statistic	Reject	Rank
1	Log-Pearson III	0.10274	No	3	0.304	No	2	0.78504	No	2
2	Normal	0.10258	No	2	0.3273	No	3	3.3501	No	5
3	Lognormal 3P	0.11105	No	4	0.34915	No	4	3.2683	No	4
4	Lognormal	0.13286	No	5	0.50872	No	5	0.55951	No	1
5	Gumbel Max	0.15675	No	6	0.81216	No	6	3.827	No	6
6	GEV	0.09487	No	1	0.30276	No	1	1.8772	No	3

Note: Rank 1 indicates the best fitting distribution; the highest rank indicates the worst fitting among the distributions.

3 Results and Discussion

3.1 Model's Overall Performance for the Calibration and Validation Period

Table 7 presents the values of NSE, PBIAS, and RSR at a station for both calibration and validation periods. According to Moriasi et al. [38], a model is considered satisfactory if it achieves NSE greater than 0.5, along with a PBIAS of less than ±20%, and RSR less than 0.7. Since we have exceeded all these thresholds, our model performance is considered to be acceptable. The NSE values of 0.69 for calibration and 0.71 for validation, along with RSR values of 0.55 and 0.53, respectively indicate good model performance in both phases, and similarly, the PBIAS values of 17.1% for calibration and 11% for validation suggest satisfactory to good performance.

Table 7. Model calibration and validation statistics for Sangutar station.

Period	**Calibration** (1982–1984)	**Validation** (1985–1986)	**Model performance**
NSE	0.69	0.71	Good
RSR	0.55	0.53	Good
PBIAS	17.1%	11%	Satisfactory, Good

Figure 4 depicts the daily hydrograph of the DHM's Hydrological Station 660, which demonstrates a close

alignment in the timing of peak observed discharges and simulated discharges. Additionally, the peaks of precipitation events and the corresponding simulated discharge occurrences also show a strong correlation.

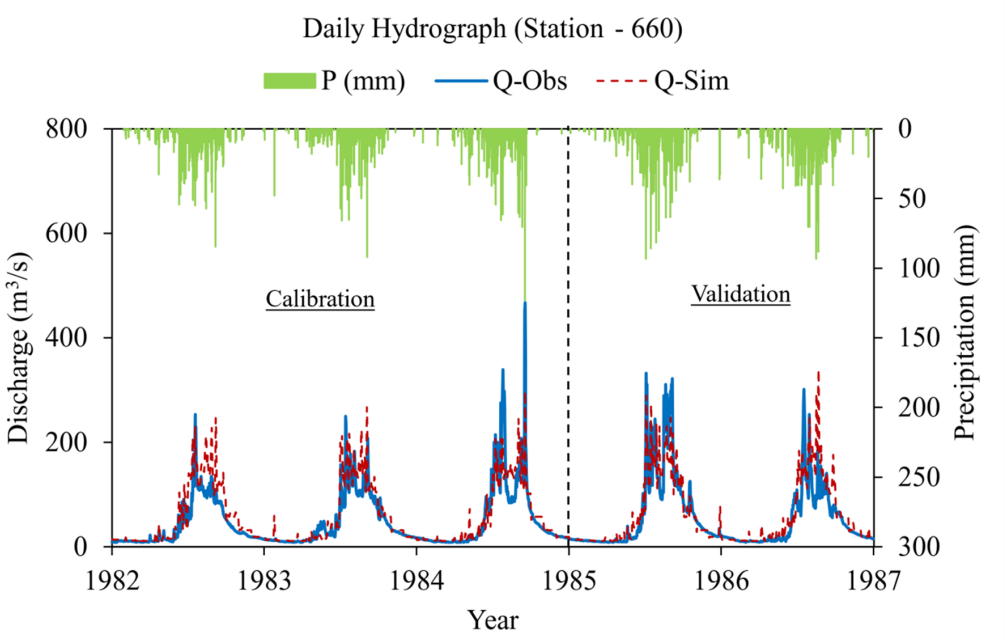

Figure 4. Calibration & validation hydrographs at daily time step.

Figure 5 presents the flow duration curve, where the high-flow segment (left side) corresponds to peak flows, typically associated with storm events or floods, while the low flow segment (right side) represents dry periods, which are critical for evaluating water availability during droughts. The simulated discharge underestimates the peak flows, suggesting that the model may not accurately capture extreme flow events. However, the base flow in the simulation aligns well with the observed data, indicating that the model accurately simulates lower flow conditions. In the 5–25% probability of exceedance range, the simulated discharge exceeds the observed values, implying that the model overestimates flows in this range compared to actual conditions.

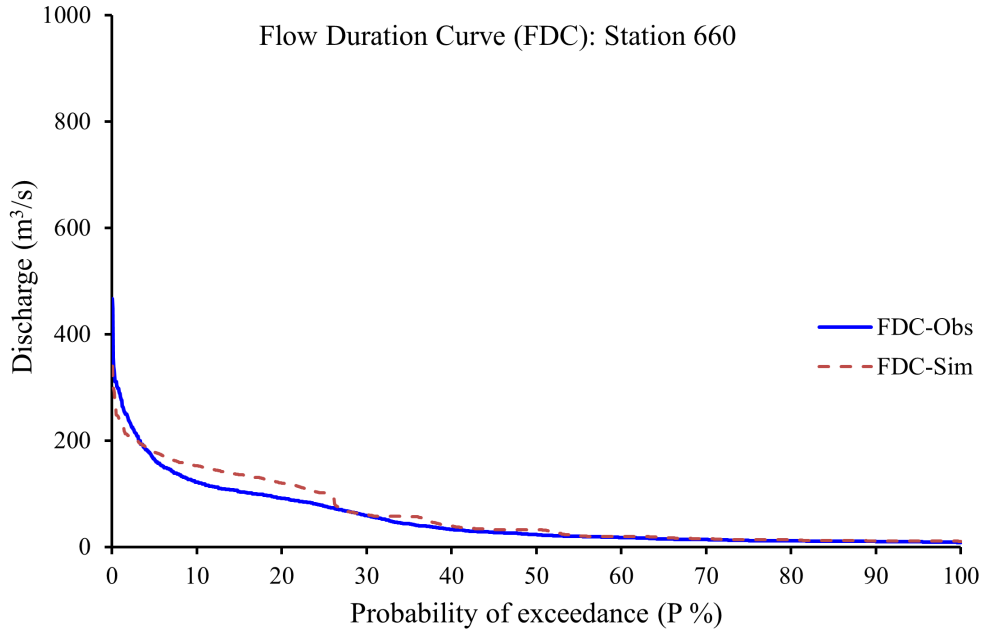

Figure 5. Flow duration curve at Station 660.

The scatter plots comparing the simulated discharge values generated by the HEC-HMS model with observed discharge data at Station 660 provide insights into the model's performance at daily and monthly time scales. For daily simulations, the regression equation $y = 0.9962x$ suggests that the model closely follows the observed discharge values, though it slightly underestimates higher flows. Additionally, the coefficient of determination (R^2) for the daily simulation is 0.8533, which indicates a strong correlation.

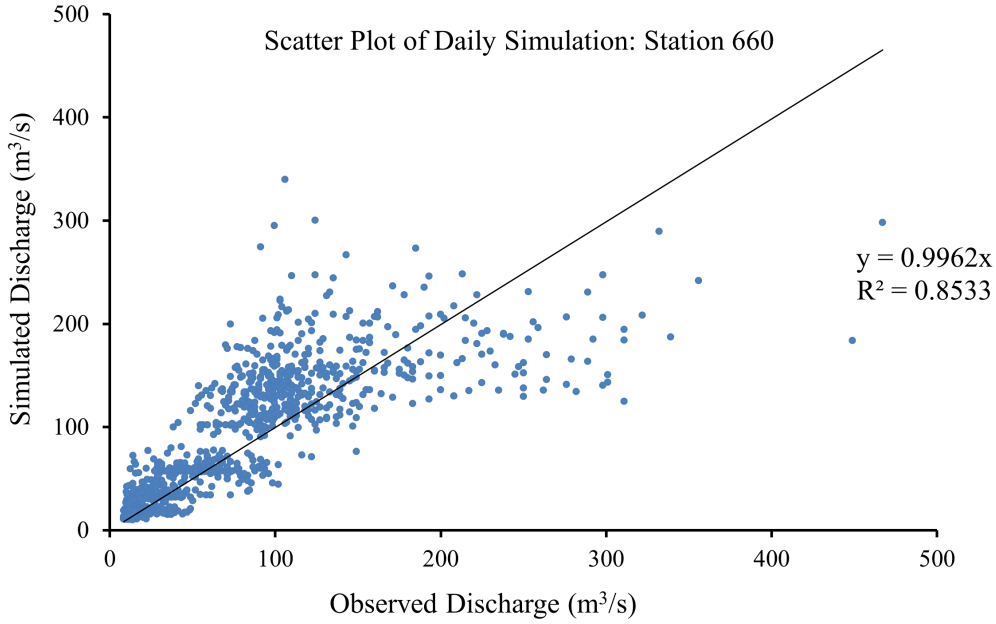

Figure 6. Scatter plot of daily simulation.

3.2 Flood Frequency Analysis

The flood frequency analysis for the Likhu Basin shows a marked rise in extreme flood events between 2025 and 2100. The 100-year flood magnitude, estimated at 474 m^3/s, is projected to occur much more frequently in future periods. Under the moderate-emission scenario (SSP 245), such events may recur every 25 years in the near and mid-future, and every 10 years by the late century. Under the high-emission scenario (SSP 585), the recurrence shortens further, with 100-year floods expected every 25 years in the near term, every 10 years in mid-century, and as often as every 5 years in the far future. Although some variability exists among climate models, the overall trend consistently indicates higher flood frequency and magnitude, particularly under SSP 585. In contrast, the moderate-emission scenario of SSP 245 demonstrates fewer extreme flood occurrences. Global Climate Models (GCMs) consistently project more frequent and intense 100-year flood events; however, there is notable variability among individual models, with ACCESS-ESM1-5 and CanESM5 projecting higher magnitudes under SSP 245, while INM-CM4-8 consistently predicts lower values. A key limitation is observed in the ensemble model, which underestimates flood risk by projecting no 100-year flood events across future scenarios, making it less reliable for detailed analysis.

Table 8. Frequency of exceedance of the 100-year return-period flood threshold.

GCM	Scenario	NF	MF	FF
ACCESS-ESM1-5	SSP 245	5	7	9
	SSP 585	3	11	40
BCC-CSM2-MR	SSP 245	2	1	0
	SSP 585	0	9	10
CanESM5	SSP 245	6	3	3
	SSP 585	11	12	31
EC-Earth3-Veg	SSP 245	2	0	1
	SSP 585	1	5	45
INM-CM4-8	SSP 245	0	1	0
	SSP 585	4	2	3
Ensemble	SSP 245	0	0	0
	SSP 585	0	0	0

NF, near future (2025–2050); MF, mid future (2051–2075); FF, far future (2076–2100).

Our findings also present a substantial rise in extreme flood occurrences and greater flood risk associated with higher emissions. This finding is supported by numerous studies conducted across diverse regions that have also demonstrated that higher emissions scenarios (i.e. RCP 8.5 or SSP 585) consistently foresee a rise in extreme events. Abuzwidah et al. [39], for instance, concluded that the SSP585 scenario projects a significantly higher level of flood risk compared to SSP245 in the UAE. Similarly, the results for the Nippersink Creek Watershed showed a 110% increase in the 100-year flood for RCP8.5 [40]. Likewise, Garg and Mishra [41] revealed that the frequency of flood events is higher under RCP 8.5 in comparison to RCP 2.6 in the Godavari River basin, India. In the Kokcha River, Afghanistan, the flood frequency analysis showed higher projected return levels for the SSP585 scenario compared to SSP245 [42]. These indicate that our findings are consistent with the results from previous similar research conducted across the world.

Daily flood discharge estimated using Log-Pearson Type III distribution under the SSP 245 suggests that the 100-year flood event (474 m^3/s) is likely to occur approximately every 25 years in the NF and MF, and every 10 years in the FF for most of the GCMs. Similarly, under SSP 585, the 100-year daily flooding event is

anticipated to trigger every 25 years in the NF, every 10 years in the MF, and every 5 years in the FF for the majority of the GCMs. Furthermore, a similar pattern of increasing flood magnitude has been showcased by GEV distribution.

Research conducted across various river basins worldwide has demonstrated consistent reduction in flood return period and increase in flood magnitude due to climate change. Iqbal et al. [43], for instance, analysed flood frequency and intensity in the Kabul basin and revealed that flood events, currently considered as 1 in 50 years, could be reduced to 1 in every 3 years to 1 in every 24 years. Similarly, in many parts of western and eastern Europe, the 100-year return period flood is likely to decrease to 50 years or less [44]. At the global level, the historical 50-year flood event is anticipated to decrease to a range of 35–45 years across different SSPs [45]. Moreover, the 20th century 100-year flood event is projected to shorten to about 10–50 years across large areas of South Asia, Southeast Asia, Northeast Eurasia, eastern and low-latitude Africa, and South America in the 21st century, which is caused by a 10–30% increase in flood discharge [46].

Based on our findings, it can be inferred that climate change is anticipated to alter flood regimes. Rising temperatures can rapidly melt snow [47] or can lead to a greater proportion of precipitation falling as rain rather than snow, which can trigger flooding [48]. Likewise, a warmer climate increases the concentration of atmospheric water vapor in proportion to the saturation concentration adhering to the Clausius-Clapeyron relationship at a rate of about 6–7% per degree rise in temperature [49, 50]. As such, the intensity of extreme precipitation is expected to increase in a warming climate, which in turn impacts the magnitude and frequency of floods [44, 51, 52]. Similarly, factors such as land-use and land-cover characteristics, antecedent soil moisture, river and catchment engineering, snow, vegetation, etc. also govern river floods [53]. However, extreme precipitation can be considered as the dominant factor in a country like Nepal where 80% of the annual rainfall is concentrated in the monsoon season [54]. Apart from extreme precipitation, precipitation that persists for prolonged duration during monsoon season may also cause river flow to surpass a threshold, resulting in flooding [55]. Additionally, increased precipitation duration and intensity may exacerbate flooding by saturating soil, thereby lowering water absorption capacity and increasing runoff.

The implications for Nepal are profound: as one of the most flood-prone countries in South Asia, the nation faces rising threats of disaster, greater risks to hydropower infrastructure, and increasing social and economic vulnerability. These findings stress the urgent need for robust flood mitigation strategies, climate-resilient planning, and the careful use of multiple climate models to reduce risks and protect both communities and water resources.

The findings highlight the urgent need to revise current design standards for hydraulic structures, as the assumption of hydrological stationarity is no longer valid under changing climate conditions [56]. Policymakers, particularly within Nepal's Departments of Roads, Irrigation, and Water Supply, should incorporate climate-adjusted design flood estimates into infrastructure planning codes and environmental impact assessment frameworks. Investment in early warning systems and real-time flood monitoring networks along medium-sized river basins, alongside strengthened land-use zoning to restrict development in flood-prone riparian zones, are recommended as priority adaptive measures.

The projected shortening of the 100-year flood recurrence interval to as few as 5 years under SSP585 poses serious risks to bridges, road crossings, and run-of-river hydropower infrastructure, including the Lower Likhu Hydropower Dam, where increased peak discharges will elevate sediment loads, turbine stress, and overtopping risk [10, 57]. Riverside communities and agricultural lands in the lower basin face growing exposure to inundation, with cascading socioeconomic consequences including livelihood disruption and displacement [3, 8]. These impacts collectively underscore the need for a coordinated, cross-sectoral climate

adaptation strategy spanning water resources, transport, energy, and social welfare planning in Nepal's mid-hill river basins.

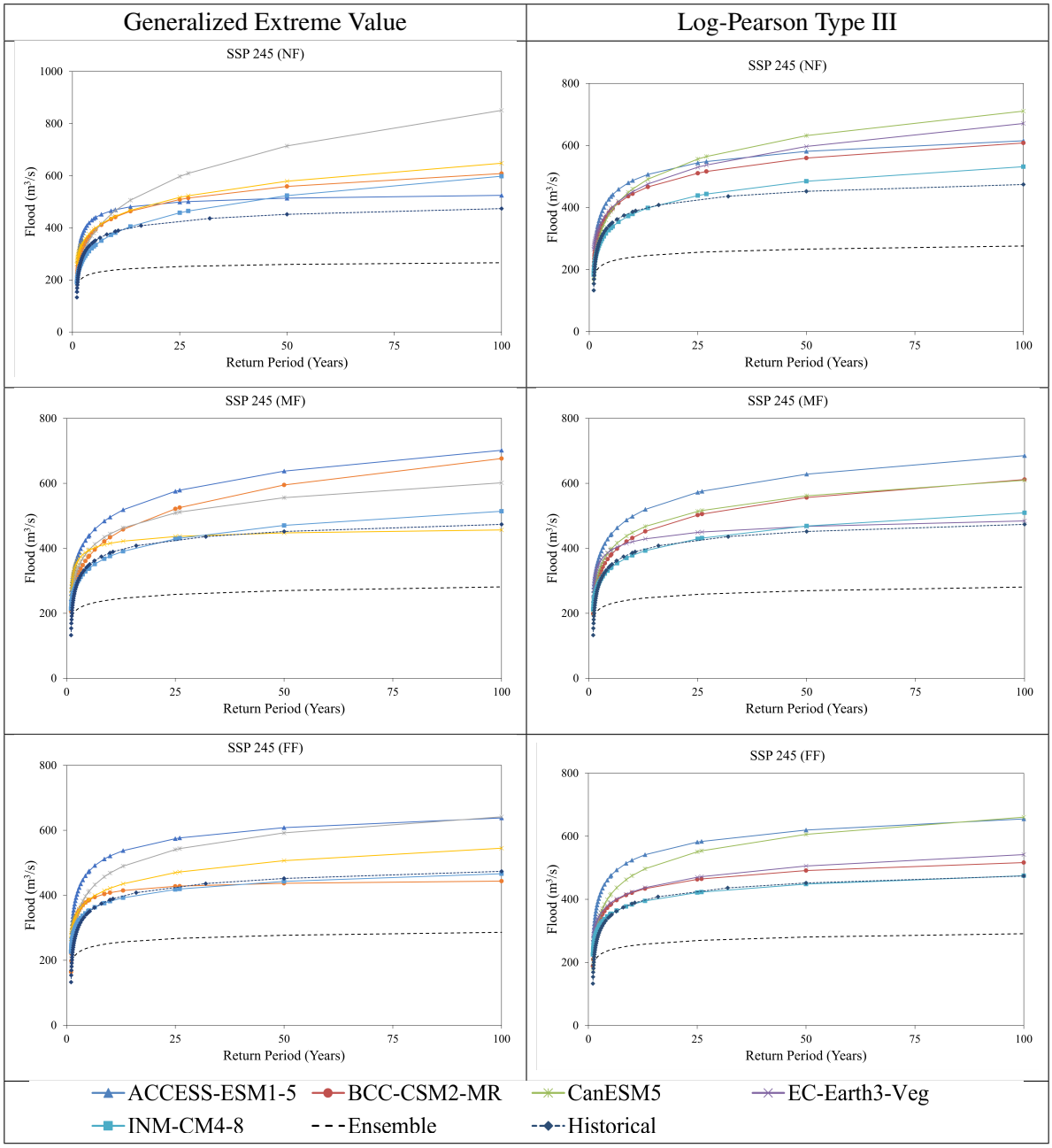

Figure 7. Plot of return period vs. flood for generalized extreme value and log-Pearson type III under SSP245.

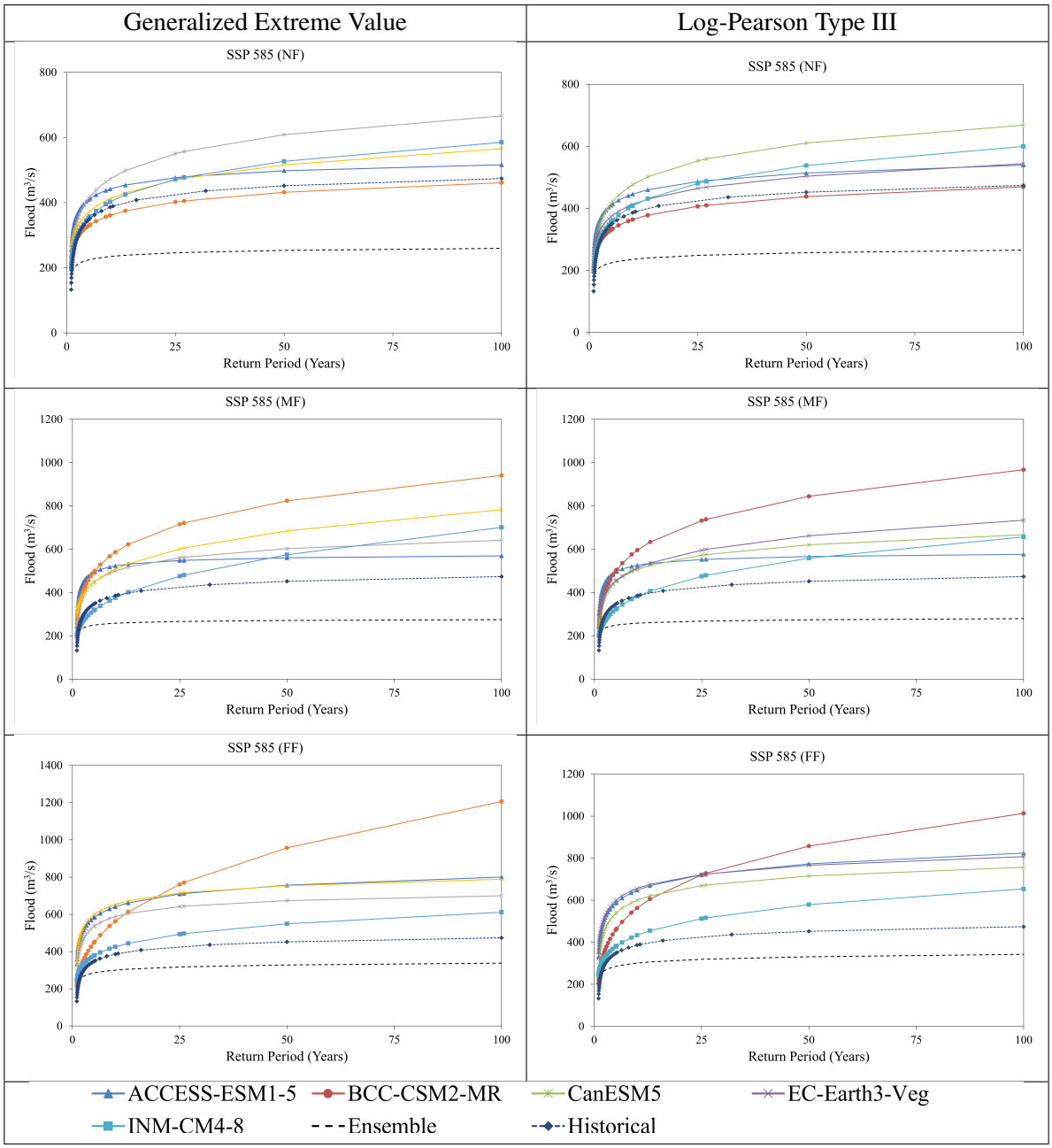

Figure 8. Plot of return period vs. flood for generalized extreme value and log-Pearson type III under SSP585.

3.3 Use of Individual GCMs

The results reveal considerable variability among individual GCMs in projected flood magnitudes and frequencies. Under SSP245, ACCESS-ESM1-5 and CanESM5 simulate higher flood magnitudes compared to the remaining models, whereas INM-CM4-8 consistently produces the lowest projections. This divergence is more pronounced under SSP585, where ACCESS-ESM1-5, CanESM5, and EC-Earth3-Veg project substantially higher flood frequencies compared to BCC-CSM2-MR and INM-CM4-8 (Figures 7 and 8). Such inter-model variability underscores the necessity of employing multiple GCMs to capture the full spectrum of uncertainty in flood projections, rather than relying on any single model.

The Ensemble Model, constructed by averaging the outputs of the five selected GCMs, consistently underestimates flood magnitudes across all scenarios and time periods, projecting zero exceedances of the 100-year flood threshold in all cases (Table 8). This behavior is a direct statistical consequence of the averaging process: when annual maximum discharges from multiple GCMs are averaged prior to frequency analysis, the extreme upper tails of the individual flow distributions are systematically dampened. Since 100-year flood events by definition reside in these tails, the ensemble mean suppresses precisely the values that are most hydrologically significant. The predicted floods under all individual GCMs consistently exceed those of the Ensemble Model, confirming that the averaging process reduces the representation of extreme events rather than providing a conservative but realistic central estimate. This finding is consistent with Devkota et al. [58], who demonstrated that floods of any given return period derived from ensembled streamflow series are systematically underestimated relative to those derived from individual climate model conditions, and concluded that ensemble-mean flows should not be used for flood estimation. Accordingly, individual GCM outputs are recommended for flood frequency analysis in this and similar basins, with the inter-model spread serving as a measure of projection uncertainty rather than the ensemble mean.

4 Conclusions

This study shows that climate change is expected to increase both the magnitude and frequency of floods in the Likhu River Catchment, especially under the high-emission SSP585 scenario. The historical 100-year flood of 474 m^3/s may no longer represent a rare event under future climate conditions; instead, it may recur within approximately 5 to 25 years depending on the climate model, scenario, and future period considered. This finding indicates that flood estimates based only on historical records are insufficient for long-term flood-risk assessment and infrastructure design.

The projected increase in flood frequency reflects a clear shift in hydrological extremes, mainly associated with changes in precipitation variability and rising temperature. The results also show substantial differences among the selected GCMs, confirming that multiple climate models should be used to represent the range of future flood uncertainty. In contrast, the Ensemble Model consistently produces lower flood magnitudes than the individual GCMs and is therefore less suitable for detailed flood-frequency estimation in this basin.

These findings have important implications for water-resource management, hydraulic-structure design, and disaster-risk reduction in the Likhu River Basin and in similar small to medium-sized Himalayan catchments. Current design standards should be revised to include climate-adjusted flood estimates, because traditional flood-frequency analyses based only on past observations may underestimate future flood hazards. Engineers, planners, and policymakers should therefore incorporate multiple GCM-based projections into the planning of bridges, hydropower facilities, irrigation structures, and other water-related infrastructure.

A key limitation of this study is the short observational record available at Station 660, which constrained the calibration and validation period to five years. This limitation reflects the broader lack of long-term hydrometeorological monitoring in Nepal's rural mid-hill and mountain river basins [8]. Although the model performance statistics indicate acceptable simulation quality, longer observational datasets would improve parameter robustness and reduce uncertainty associated with model calibration [59]. Future studies should combine improved ground-based observations with satellite-derived precipitation products, such as CHIRPS or GPM-IMERG, to support more reliable climate-impact assessments in data-scarce Himalayan basins [10].

References

[1] L. Wang, S. Cui, Y. Li, et al. A review of the flood management: from flood control to flood resilience. *Heliyon*, 8(11):e11763, 2022.

[2] E. Yalcin. Assessing future changes in flood frequencies under cmip6 climate projections using swat modeling: a case study of bitlis creek, turkey. *Journal of Water and Climate Change*, 15(5):2212–2231, 2024.

[3] UNDRR. Human cost of disasters: an overview of the last 20 years 2000–2019. Technical report, United Nations Office for Disaster Risk Reduction, Geneva, Switzerland, 2020.

[4] Centre for Research on the Epidemiology of Disasters (CRED). 2024 disasters in numbers. Technical report, Centre for Research on the Epidemiology of Disasters (CRED), Brussels, Belgium, 2025.

[5] Sukanya and S. Joseph. Climate change impacts on water resources: An overview. In *Visualization Techniques for Climate Change with Machine Learning and Artificial Intelligence*, pages 55–76. CRC Press, 2023.

[6] A. Becker and U. Grunewald. Flood risk in central europe. *Science*, 300(5622):1099, 2003.

[7] IPCC. Climate change 2023: Synthesis report. Technical report, IPCC, Geneva, 2023.

[8] B. R. Shrestha, R. K. Rai, and S. Marasini. Review of flood hazards studies in nepal. *The Geographic Base*, 7:24–32, 2020.

[9] A. F. Lutz, W. W. Immerzeel, A. B. Shrestha, and M. F. P. Bierkens. Consistent increase in high asia's runoff due to increasing glacier melt and precipitation. *Nature Climate Change*, 4(7):587–592, 2014.

[10] L. Bharati, P. Gurung, P. Jayakody, V. Smakhtin, and U. Bhattarai. The projected impact of climate change on water availability and development in the koshi basin, nepal. *Mountain Research and Development*, 34(2):118–130, 2014.

[11] Practical Action. *Temporal and spatial variability of climate change over Nepal (1976–2005)*. Practical Action Nepal, Kathmandu, 2009.

[12] MoHA. Nepal disaster report 2024: focus on reconstruction and resilience. Technical report, Ministry of Home Affairs, Government of Nepal, 2024.

[13] M. R. Kafle. Rainfall-runoff modelling of koshi river basin using hec-hms. *Journal of Hydrogeology & Hydrologic Engineering*, 8(1), 2019.

[14] A. Bhattarai, U. Bhattarai, K. R. Maharjan, and L. P. Devkota. Assessing the characteristics of extreme floods in nepal. *PIAHS*, 387:3–8, 2024.

[15] B. Acharya and B. Joshi. Flood frequency analysis for an ungauged himalayan river basin using different methods: a case study of modi khola, parbat, nepal. *Meteorology Hydrology and Water Management*, 8 (2):46–51, 2020.

[16] S. Fahad and J. Wang. Climate change, vulnerability, and its impacts in rural pakistan: a review. *Environmental Science and Pollution Research*, 27(2):1334–1338, 2020.

[17] N. Chokkavarapu and V. R. Mandla. Comparative study of gcms, rcms, downscaling and hydrological models. *SN Applied Sciences*, 1(12), 2019.

[18] A. Izzaddin, A. Langousis, V. Totaro, M. Yaseen, and V. Iacobellis. A new diagram for performance evaluation of complex models. *Stochastic Environmental Research and Risk Assessment*, 38(6): 2261–2281, 2024.

[19] C. L. Chidi, B. R. Shrestha, and L. Sapkota. Flood risk mapping and analysis: A case study of andheri khola catchment, sindhuli district, nepal. *Geographical Journal of Nepal*, pages 103–118, 2022.

[20] H. Sheng, X. Xu, J. H. Gao, et al. Frequency and magnitude variability of yalu river flooding: numerical analyses for the last 1000 years. *Hydrology and Earth System Sciences*, 24:4743–4761, 2020.

[21] E. Gaume, V. Bain, P. Bernardara, et al. A compilation of data on european flash floods. *Journal of Hydrology*, 367(1-2):70–78, 2009.

[22] M. Borga, P. Boscolo, F. Zanon, and M. Sangati. Hydrometeorological analysis of the august 29, 2003 flash flood in the eastern italian alps. *Journal of Hydrometeorology*, 8(5):1049–1067, 2007.

[23] W. W. Immerzeel, L. P. H. van Beek, and M. F. P. Bierkens. Climate change will affect the asian water towers. *Science*, 328(5984):1382–1385, 2010.

[24] S. R. Chalise, S. R. Kansakar, G. Rees, et al. Management of water resources and low flow estimation for the himalayan basins of nepal. *Journal of Hydrology*, 282(1–4):25–35, 2003.

[25] U.S. Army Corps of Engineers. *Hydrologic Modeling System HEC-HMS: Technical Reference Manual*. Hydrologic Engineering Center, 2023. Version 4.11.

[26] C. Teutschbein and J. Seibert. Bias correction of regional climate model simulations for hydrological climate-change impact studies. *Journal of Hydrology*, 456–457:12–29, 2012.

[27] D. N. Moriasi, J. G. Arnold, Liew M. W. Van, R. L. Bingner, R. D. Harmel, and T. L. Veith. Model evaluation guidelines for watershed simulations. *Transactions of the ASABE*, 50(3):885–900, 2007.

[28] V. Mishra, U. Bhatia, and A. D. Tiwari. Bias-corrected climate projections for south asia from cmip6. *Scientific Data*, 7(1):338, 2020.

[29] K. Baral, V. P. Pandey, and A. M. S. Pradhan. Impact on hydrological alteration due to climate change in seti watershed. *Journal of UTEC Engineering Management*, 2(01):25–35, 2024.

[30] B. J. Cisneros, T. Oki, N. W. Arnell, G. Benito, J. G. Cogley, P. Doll, T. Jiang, and S. S. Mwakalila. *Climate Change 2014: impacts, adaptation, and vulnerability*. Cambridge University Press, 2014.

[31] S. L. Grotch and M. C. MacCracken. The use of general circulation models to predict regional climatic change. *Journal of Climate*, 4(3):286–303, 1991.

[32] L. Gudmundsson, J. B. Bremnes, J. E. Haugen, and T. Engen-Skaugen. Technical note: Downscaling rcm precipitation to the station scale using statistical transformations—a comparison of methods. *Hydrology and Earth System Sciences*, 16(9):3383–3390, 2012.

[33] J. Chen, F. P. Brissette, D. Chaumont, and M. Braun. Finding appropriate bias correction methods in downscaling precipitation for hydrologic impact studies over north america. *Water Resources Research*, 49(7):4187–4205, 2013.

[34] J. C. Refsgaard and J. Knudsen. Operational validation and intercomparison of different types of hydrological models. *Water Resources Research*, 32(7):2189–2202, 1996.

[35] G. Tegegne, D. K. Park, and Y. O. Kim. Comparison of hydrological models for the assessment of water resources in a data-scarce region, the upper blue nile river basin. *Journal of Hydrology: Regional Studies*, 14:49–66, 2017.

[36] C. Perrin, L. Oudin, V. Andreassian, C. Rojas-Serna, C. Michel, and T. Mathevet. Impact of limited streamflow data on the efficiency and the parameters of rainfall–runoff models. *Hydrological Sciences Journal*, 52(1):131–151, 2007.

[37] K. Schittkowski. Easy-fit: a software system for data fitting in dynamical systems. *Structural and Multidisciplinary Optimization*, 23(2):153–169, 2002.

[38] D. N. Moriasi, M. W. Gitau, N. Pai, and P. Daggupati. Hydrologic and water quality models: performance measures and evaluation criteria. *Transactions of the ASABE*, 58:1763–1785, 2015.

[39] M. Abuzwidah, A. Elawady, A. G. Ashour, A. G. Yilmaz, A. Shanableh, and W. Zeiada. Flood risk assessment for sustainable transportation planning and development under climate change: A gis-based comparative analysis of cmip6 scenarios. *Sustainability*, 16(14):5939, 2024.

[40] Y. Bai, Z. Zhang, and W. Zhao. Assessing the impact of climate change on flood events using hec-hms and cmip5. *Water, Air, and Soil Pollution*, 230(6), 2019.

[41] S. Garg and V. Mishra. Role of extreme precipitation and initial hydrologic conditions on floods in godavari basin. *Water Resources Research*, 55(11):9191–9210, 2019.

[42] H. Shams, A. Khan, K. Haleem, and S. Mahmood. Assessing the effects of climate and land-use change on flood recurrence in kokcha river, afghanistan. *Journal of Water and Climate Change*, 15(5): 2464–2483, 2024.

[43] M. Iqbal, Z. Dahri, E. Querner, A. Khan, and N. Hofstra. Impact of climate change on flood frequency and intensity in the kabul river basin. *Geosciences*, 8(4):114, 2018.

[44] R. Dankers and L. Feyen. Climate change impact on flood hazard in europe. *Journal of Geophysical Research*, 113(D19), 2008.

[45] X. Huang, J. Yin, L. J. Slater, S. Kang, S. He, and P. Liu. Global projection of flood risk with a bivariate framework under 1.5–3.0°c warming levels. *Earth's Future*, 12(4), 2024.

[46] Y. Hirabayashi, R. Mahendran, S. Koirala, et al. Global flood risk under climate change. *Nature Climate Change*, 3(9):816–821, 2013.

[47] J. W. Pomeroy, R. E. Stewart, and P. H. Whitfield. The 2013 flood event in the south saskatchewan and elk river basins. *Canadian Water Resources Journal*, 41(1–2):105–117, 2016.

[48] K. N. Musselman, F. Lehner, K. Ikeda, et al. Projected increases and shifts in rain-on-snow flood risk over western north america. *Nature Climate Change*, 8(9):808–812, 2018.

[49] M. R. Allen and W. J. Ingram. Constraints on future changes in climate and the hydrologic cycle. *Nature*, 419(6903):224–232, 2002.

[50] W. Ingram. Increases all round: Extreme precipitation. *Nature Climate Change*, 6(5):443–444, 2016.

[51] W. R. Berghuijs, R. A. Woods, C. J. Hutton, and M. Sivapalan. Dominant flood generating mechanisms across the united states. *Geophysical Research Letters*, 43(9):4382–4390, 2016.

[52] K. E. Trenberth, A. Dai, R. M. Rasmussen, and B. Parsons. The changing character of precipitation. *Bull. Am. Meteorol. Soc.*, 84:1205–1217, 2003.

[53] IPCC. *Climate Change 2021: The Physical Science Basis*. Cambridge University Press, 2021.

[54] M. M. Q. Mirza. Climate change, flooding in south asia and implications. *Regional Environmental Change*, 11(S1):95–107, 2011.

[55] D. Aryal, L. Wang, T. R. Adhikari, J. Zhou, X. Li, M. Shrestha, Y. Wang, and D. Chen. A model-based flood hazard mapping on the southern slope of himalaya. *Water*, 12(2):540, 2020.

[56] P. C. D. Milly, Julio Betancourt, Malin Falkenmark, Robert M. Hirsch, Zbigniew W. Kundzewicz, Dennis P. Lettenmaier, and Ronald J. Stouffer. Stationarity is dead: Whither water management? *Science*, 319(5863):573–574, 2008. doi: 10.1126/science.1151915.

[57] Byman Hamududu and Aanund Killingtveit. Assessing climate change impacts on global hydropower. *Energies*, 5(2):305–322, 2012. doi: 10.3390/en5020305.

[58] L. P. Devkota, U. Bhattarai, R. Devkota, T. Maraseni, and S. Marahatta. Questioning ensembles versus individual climate model generated flows. *Journal of Flood Risk Management*, 17:e12978, 2024.

[59] K. Beven. Changing ideas in hydrology—the case of physically-based models. *Journal of Hydrology*, 105:157–172, 1989.